TECHNICAL MEMORANDUM

370

Westerly wind events and the 1997 El-Niño event in the ECMWF seasonal forecasting system: a case study

Magdalena Alonso Balmaseda, Frédéric Vitart, Laura Ferranti, David Anderson.

Research Department

11 September 2002

European Centre for Medium-Range Weather Forecasts
Europäisches Zentrum für mittelfristige Wettervorhersage
Centre européen pour les prévisions météorologiques à moyen terme

For additional copies please contact

The Library
ECMWF
Shinfield Park
Reading
RG2 9AX
library@ecmwf.int

Series: ECMWF Technical Memoranda

A full list of ECMWF Publications can be found on our web site under:
http://www.ecmwf.int/publications/

Abstract

The 1997-1998 El-Niño was one of the strongest on record. Its onset was predicted by several numerical models, though none fully captured its intensity. This was the case for the ECMWF seasonal forecasting system which underestimated the intensification during the period June-July 1997 by more than 1K. Several strong westerly wind events developed during the onset of the 1997-1998 El-Niño suggesting that westerly wind events played a key role in the intensification of this El-Niño. The present paper quantifies the impact of westerly wind events on the 1997-1998 El-Niño in the ECMWF seasonal forecasting system, through a series of experiments in which various modifications are made to convective parameterization and wind forcing to increase wind variability in the western Pacific.

The first modification to the coupled model involves adding observed wind anomalies to the wind stress derived from the atmospheric model before they are used to force the oceanic component of the coupled model. Results indicate that the westerly wind event that occurred in May-June 1997 may have accounted for a warming of more than 0.5K in the NINO3 region. The second modification, involves adding stochastic perturbations to the model tendencies. This produces an increase in the spread of the ensemble and a slightly better forecast of NINO3 sea surface temperatures (SSTs). In a third set of experiments, the convective parameterization of the atmospheric model was modified in order to allow more convective available potential energy to accumulate before convection is triggered. This leads to both a significant improvement in the simulation of westerly wind events and in the prediction of the NINO3 SSTs. A few members of the ensemble produce a warming in the NINO3 region comparable to the warming produced by the observed westerly wind burst of May-June 1997.

Ocean-only experiments indicate that the response of the coupled model to the wind perturbation is smaller than that in forced mode, probably due to the strong damping effect of the induced heat flux. The different ocean mean state does not seem to be responsible for the weak coupled response in the NINO3 region. The relative importance of anomalies in zonal wind stress, heat flux, precipitation minus evaporation (P-E), and ocean initial conditions is determined.

1 Introduction

Predicting El-Niño is a topic of great interest since it is the most important source of potentially predictable interannual variability. The prediction of its occurrence and development represents a particularly challenging task for dynamical seasonal forecasting. Several models of intermediate complexity, based on a relatively simple representation of the Equatorial Pacific Ocean and the tropical atmosphere, have been applied to this topic with some success. See for example Latif et al 1998 and references therein. The performance of general circulation models to predict sea surface temperature anomalies has significantly improved in recent years and some of them provided the best real-time numerical forecasts of the 1997-1998 El-Niño (Trenberth 1998) although all the dynamical models considered by Barnston et al. (1999) underestimated the exceptional strength of the 1997-1998 El-Niño.

The ECMWF seasonal forecasting system, based on coupled General Circulation Models (GCM) integrations, was generally rather successful in predicting the occurrence of the 1997-1998 event, its maintenance and its decay, a few months in advance, but forecasts initiated in April and May underestimated its intensification in June and July 1997 by more than 1K. The main goal of the present paper is to investigate the reasons for this failure.

While the El-Niño mode explains most of the interannual variability, tropical intraseasonal variability, which can be very intense in some years, is also of interest for seasonal forecasting. For example, the strong El-Niño event of 1997 developed during a period of intense intraseasonal activity. Those variations may condition the development of warm tropical SSTs and therefore may play a substantial role in the onset and development of the El-Niño Southern Oscillation (ENSO).

The Madden Julian Oscillation (MJO) is the most dominant and coherent component of the intraseasonal variability in the tropical atmosphere (Madden and Julian 1971, 1972). When it is active it represents a substantial modulation of the convective activity over the Indian and west Pacific Oceans. Kessler and Kleeman (2000) suggest that the MJO may influence the tropical climate by modulating the timing and strength of ENSO events. Strong MJOs have been observed prior to and during the onset of recent ENSO events, and Kelvin waves generated by MJO forcing in the western Pacific can lead to an increase of sea surface temperatures in the tropical eastern Pacific. However, the impact of MJOs on ENSO is still questionable since the evidence for a significant statistical relationship between large-scale MJO activity and ENSO is somewhat contradictory (Hendon et al. 1998; Slingo et al. 1998; Bergman et al. 2001; Benestad et al. 2002).

Rapid changes in surface winds over the Indonesian region, known as Westerly Wind Bursts (see for instance Harrison and Giese, 1991) are observed on the intraseasonal time scale. The amplitude of the zonal wind anomaly is of the order of a few meters per second. It is still unclear to what extent westerly wind events are intimately related to the large-scale MJO phenomenon. Westerly wind events tend to develop during active phases of the MJO (Zhang 1996; Lin and Johnson 1996; Chen et al 1996), though they can also form from paired tropical cyclones (Keen 1982) and cold surges from midlatitudes (Harrison 1984). Barnett (1984) suggested that westerly wind events could affect the ENSO cycle. Slingo (1998), McPhaden (1999) and Boulanger et al. (2001) amongst others have argued that westerly wind events, possibly associated with the MJO, in late 1996 and the first half of 1997 played a crucial role in the onset and development of ENSO.

Westerly wind events were present in the western Pacific during the onset of several recent El-Niño events: 1990-91, 1992-93, 1993-94, and 1996-97 (Krishnamurti et al 2000). In 1997, before the onset of the strongest El-Niño recorded, several strong westerly winds events were observed (November 1996, December 1996, February-March 1997). Krishnamurti et al (2000) demonstrate that the initialization of a coupled GCM including westerly wind events in the ocean data assimilation significantly improved the forecasts of the 1997 El-Niño. Perigaud and Cassou (2000), using an intermediate coupled model, argue that the presence of westerly wind events can impact the development of an El-Niño event but only if the oceanic heat content is high, as was the case in 1997. Therefore, westerly wind events may be an important player in the intensification of the 1997 El-Niño event. If this is the case, then it is important for a coupled GCM to be able to generate such wind stress variability in order to successfully forecast El-Niño events months in advance.

Simulating a realistic atmospheric intraseasonal variability over the tropical Pacific is still a difficult task for state-of-the-art GCMs. As part of the Atmospheric Model Intercomparison Project (AMIP; Gates, 1992), Slingo et al. (1996) have compared the MJO variability in fifteen GCMs to the observed variability as represented by the ECMWF analyses. Their studies showed that the most consistent shortcoming among the models is the weak representation of the strength of the intraseasonal variability. The drastic lack of MJO variability west of the dateline in the GCMs may significantly affect their ability to create westerly wind events. It has therefore been hypothesized that the failure of GCMs to predict the strong intensity of the 1997-1998 El-Niño event is related to their inability to simulate realistic westerly wind events.

This study explores the above hypothesis in the context of the ECMWF seasonal forecasting system. Section 2 documents the ECMWF seasonal predictions of the 1997-1998 El-Niño, and the ability of the ECMWF coupled system to simulate realistic MJOs and westerly wind events. In Section 3, results from sensitivity experiments using fully coupled GCMs and designed to evaluate the impact of westerly wind events on the El-Niño 1997 are discussed. Section 4 shows that there is large sensitivity to a specific change in the cumulus parameterization scheme. Results from these experiments indicate that the significant improvement in predicting the SST anomalies over the NINO3 region (150W-90W, 5N-5S) for the 1997-1998 El Niño is related to the enhancement of tropical intraseasonal activity in the model. The relative importance of the wind and heat flux variability in the amplitude of SST anomalies is considered in Section 5 by means of ocean-only experiments. Summary and conclusions are presented in Section 6.

2 Seasonal predictions of NINO3 SST anomalies and simulation of intraseasonal activity

The ECMWF seasonal forecasting system (Stockdale et al 1998) is based on a coupled GCM that has been used to make an ensemble of 6-month forecasts every month from 1991 to present. The atmospheric component (IFS cycle 15R8) has a T63 spectral resolution and a 1.875^o grid for surface and physical processes; there are 31 vertical levels. The ocean resolution is comparable in mid-latitudes, but is increased in the tropics to about 0.5^o in the latitudinal direction, so as to resolve the equatorial waves which are important for El-Niño. There are 20 vertical levels of which eight are in the upper 200 meters. The atmospheric and land surface initial conditions are taken from the operational analyses/reanalyses produced by ECMWF. Ocean initial conditions are taken from an analysis of the ocean state made by forcing the ocean with the analyzed surface fluxes of momentum, fresh water and heat while assimilating all available subsurface thermal ocean data using the optimal interpolation scheme of Smith et al (1991) and relaxing to surface temperature analyses (Reynolds and Smith 1994).

The ECMWF seasonal forecasting system displays skill in predicting SST anomalies over the NINO3 region: fig 1 shows that the system was successful in forecasting the onset of the 1997 El-Niño event and its decay. For forecasts started in April and May, however, the model severely underestimated the intensity of the SST warming during the months of June and July. This result is consistent with other GCM forecasts (Barnston et al 1999, Landsea and Knaff 2000).

The period from December 1996 to June 1997 was characterized by strong tropical intraseasonal activity within which were very energetic westerly wind events (McPhaden 1999, Slingo 1998). It is likely that such strong westerly wind events perturbed significantly the equatorial ocean by creating oceanic Kelvin-waves and possibly intensifying the El-Niño (McPhaden 1999). The seasonal forecast system is generally deficient in representing tropical intraseasonal activity. In fact, westerly wind anomalies propagate eastwards only when they are present in the initial conditions. This is illustrated by Figure 2 for forecasts initiated in February and March 1997. Comparison of the analysis of fig 2a with the forecasts in fig 2b, shows that the wind events of mid-February and especially March were not reproduced in forecasts started at the beginning of February. On the other hand fig 2c shows that some aspects of the March event were captured in forecasts started on 1 March.

Figure 3a shows strong westerly wind events that developed from May to mid-June 1997 and propagated eastward from the Indian Ocean to as far east as 150W, with an intensity exceeding 0.08 Nm^{-2}. For forecasts started on 1 May 1997, not one single member of the 30-member ensemble of the ECMWF seasonal forecasting system was able to produce propagating wind events comparable to those observed. Fig 3b shows one ensemble member chosen at random from the coupled control experiment (C_control) which will be introduced in secn 3. It is not just the surface winds that do not show propagation. Fig 4a shows the velocity potential at 200 hPa in the ECMWF analysis, a field that is often used as a measure of MJO activity. Eastward propagation can be clearly seen. Fig 4b shows just one ensemble member from C_control drawn at random. No eastward propagation is evident. Analysis of other ensemble members confirms the absence of eastward propagation of MJO-like activity.

Ensembles of atmospheric-only integrations initiated with the same atmospheric initial conditions as in the coupled forecasts (from analyzed atmospheric state, soil moisture and snow cover), and driven by observed SSTs show a similar behaviour. The atmospheric simulations, integrated for several cases including May 1997 were unable to create anything close to the observed westerly wind events, except when the wind event was present in the initial conditions, suggesting that the lack of westerly wind events in the coupled model stems from a deficiency in the atmospheric model. Several atmospheric integrations have shown that increasing horizontal resolution of the atmospheric component of the GCM to T95, T159 and T319, does not improve

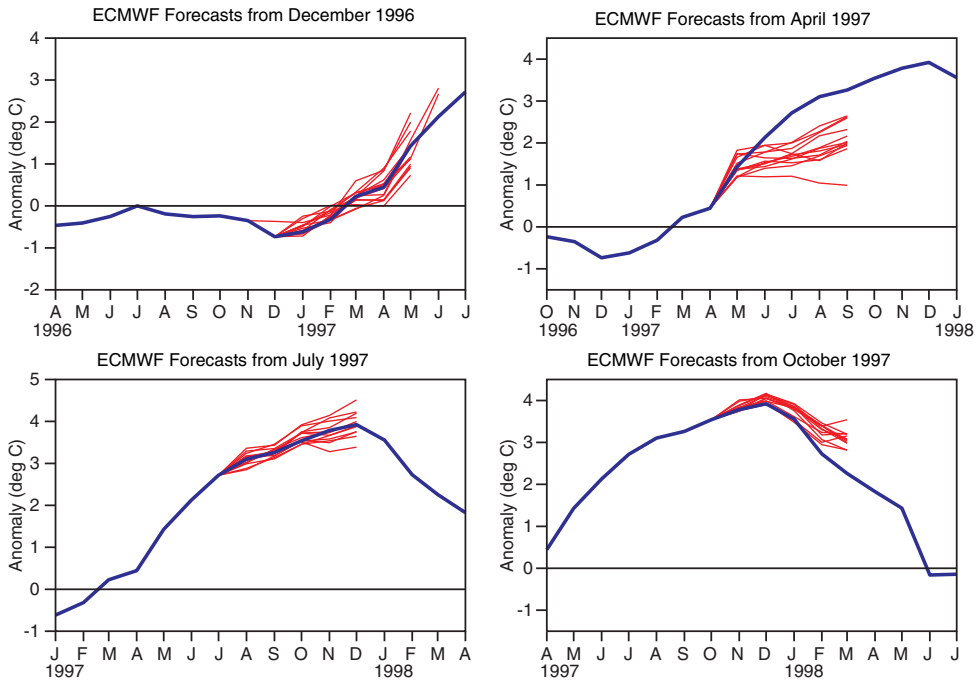

Figure 1: Plumes of monthly mean SST anomalies predicted for the NINO3 region ($5^oS - 5^oN, 90^oW - 150^oW$). Forecasts are initialized one day apart and run for 184 days. Start dates: December 1996 (top left), April 1997 (top right), July 1997 (bottom left) and October 1997 (bottom right). The thick line shows the observed values. Each thin line represents one member of the ensemble.

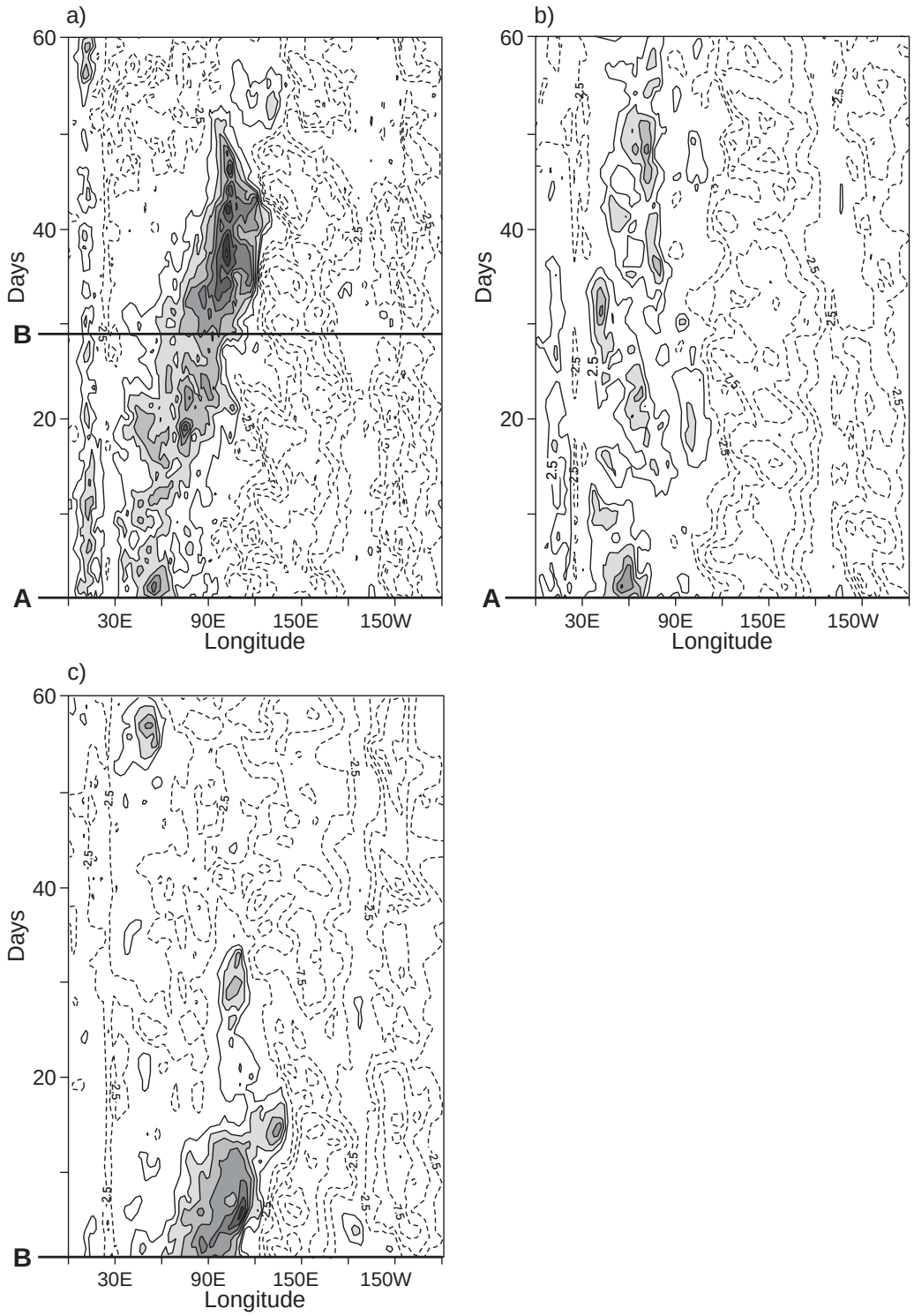

Figure 2: Time evolution of the zonal wind at 850 hPa over the tropical Indian and Pacific Oceans in a) ECMWF operational analysis from 1 February 1997 to 30 March 1997, and in one ensemble member from the operational coupled forecast system (system 1) starting on a) 1 February 1997 and c) 1 March 1997. The westerly wind burst is present in the initial conditions of the latter forecast. The zonal wind has been averaged from 10S to the Equator. The starting times of the forecasts are marked on the analysis of panel a, by A and B. The contour interval (c.i.) is 2.5m/s. Dashed lines indicate easterly winds

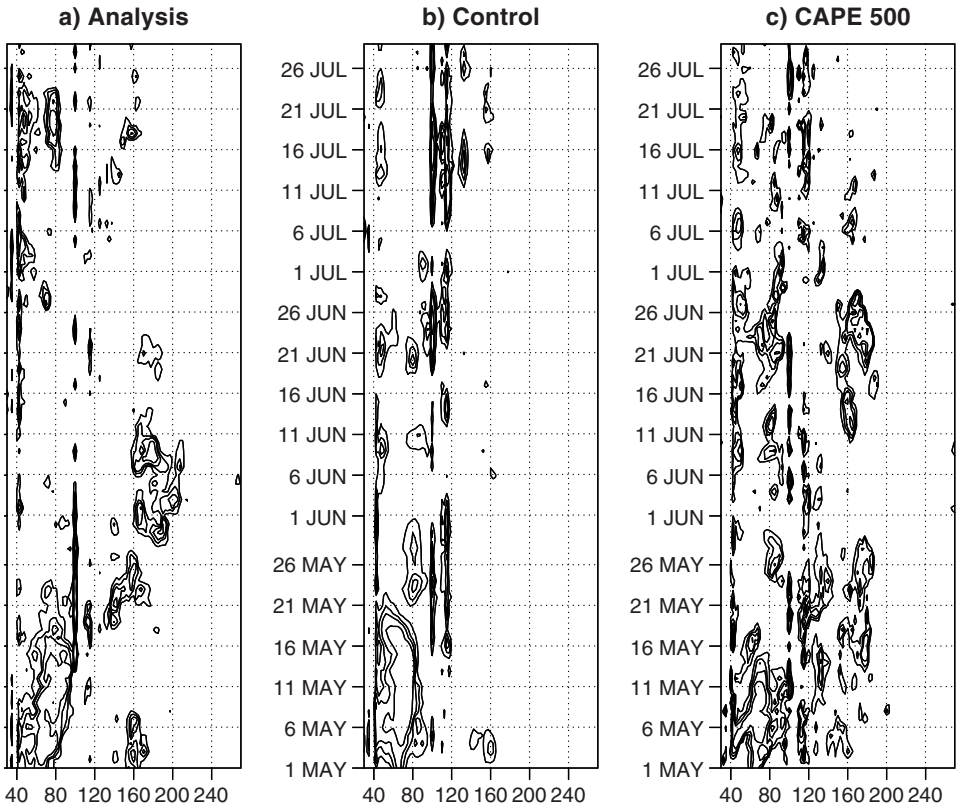

Figure 3: Time evolution of surface zonal wind stress over the tropical Indian and Pacific Oceans a) in the ECMWF operational analysis, b) an ensemble member from the C_control experiment and c) an ensemble member from the C_cape experiment. The wind stress has been averaged from 5S to 5N. Contours are 0.02, 0.04, 0.06 and 0.1Nm^{-2}. Values below 0.02 Nm^{-2} are not shown.

significantly the simulation of the intraseasonal variability of the wind stress over the tropical Pacific, indicating that the problem is not simply one of resolution.

In summary, the tropical intraseasonal activity is severely underestimated in both coupled and uncoupled simulations integrated for 30 days or longer. The model fails to simulate eastward propagation of anomalous convection from the Indian Ocean to the western and central Pacific. The variability in the western Pacific is weaker in the model compared to observations. This might indicate a deficiency in the parameterization of the physical processes related to the MJO. Below we will in fact show that the problem occurs within a rather short timescale.

At ECMWF, high resolution forecasts are made every day out to 10 days in order to generate medium range weather forecasts. These can be used to evaluate the ability of the model to simulate and predict westerly wind events up to 10 days ahead. We will concentrate on the May-June 1997 westerly wind event. Fig 5 shows 'Hovmoller' plots of the surface wind for 1-day, 2-day, 5-day and 10-day forecasts. The dates on figure 5 correspond to the verifying time of the forecast. If the model could simulate equatorial winds correctly and they were predictable, then the 10-day forecasts of fig 5d should look like the analyses- these latter are not shown but in fact the 1-day forecasts of fig 5a are a good proxy as the model does not degrade too much over the first day of integration. Fig 5 shows that the speed of propagation of the westerly wind event over the Indian Ocean gets slower as the forecast-range increases and the amplitude is noticeably reduced (compare 1-day forecasts in fig 5a with 10-day forecasts in fig 5d for instance). The model fails to predict the transition of the westerly wind event from the Indian Ocean to the western Pacific more than 2 days in advance. In particular, the model fails to predict the correct intensity of the westerly wind event over the western Pacific (between 120E and 140E) during the period 15 May-1st June 48 hours in advance (Fig 5b) and does not predict its occurrence at all over the western Pacific 5 days in advance (Fig. 5c). However, when the initial conditions include the westerly wind event in the western Pacific, the model succeeds in predicting its propagation into the central Pacific (between 160E and 140W) 10 days in advance, although it does not extend as far eastward as in the analysis (Fig 5d).

The predictability of westerly wind events on seasonal time scales is probably not very high. However, if the atmospheric model were able to create westerly wind events, one would expect that within a sufficiently large ensemble, some members of the ensemble would create a westerly wind event at approximately the right time and with the right intensity. If the June 1997 westerly wind event played a significant role in the development of the 1997 El-Niño but its predictability on the seasonal scale was low, then, even with a perfect atmospheric model, only a few members of the ensemble would be expected to predict the strong warming in the NINO3 region in June-July 1997.

3 Sensitivity of the coupled forecast to the May-June 1997 westerly wind event

Although the intraseasonal activity is largely underestimated by the seasonal forecasts throughout the period December 1996 to June 1997, we will concentrate on the specific case of seasonal predictions initiated in May 1997. The 1st May was chosen as a starting date partly because the operational seasonal forecasts from May failed to predict the intensity of the El-Niño and partly because it is close to the observed May-June westerly wind event. By performing additional experiments we will investigate whether part of the seasonal prediction error could be related to the inadequate representation of westerly wind activity.

All the experiments have been performed using the same ocean component of the coupled GCM as in the operational seasonal forecasting system but with a more recent version of the atmospheric model (known as cycle 19r1). A 5-member ensemble of 3-month integrations has been generated, in which each one is started on 1 May for each year from 91-96. These are used to create the reference climatology (C_CONTROL_CLIM)

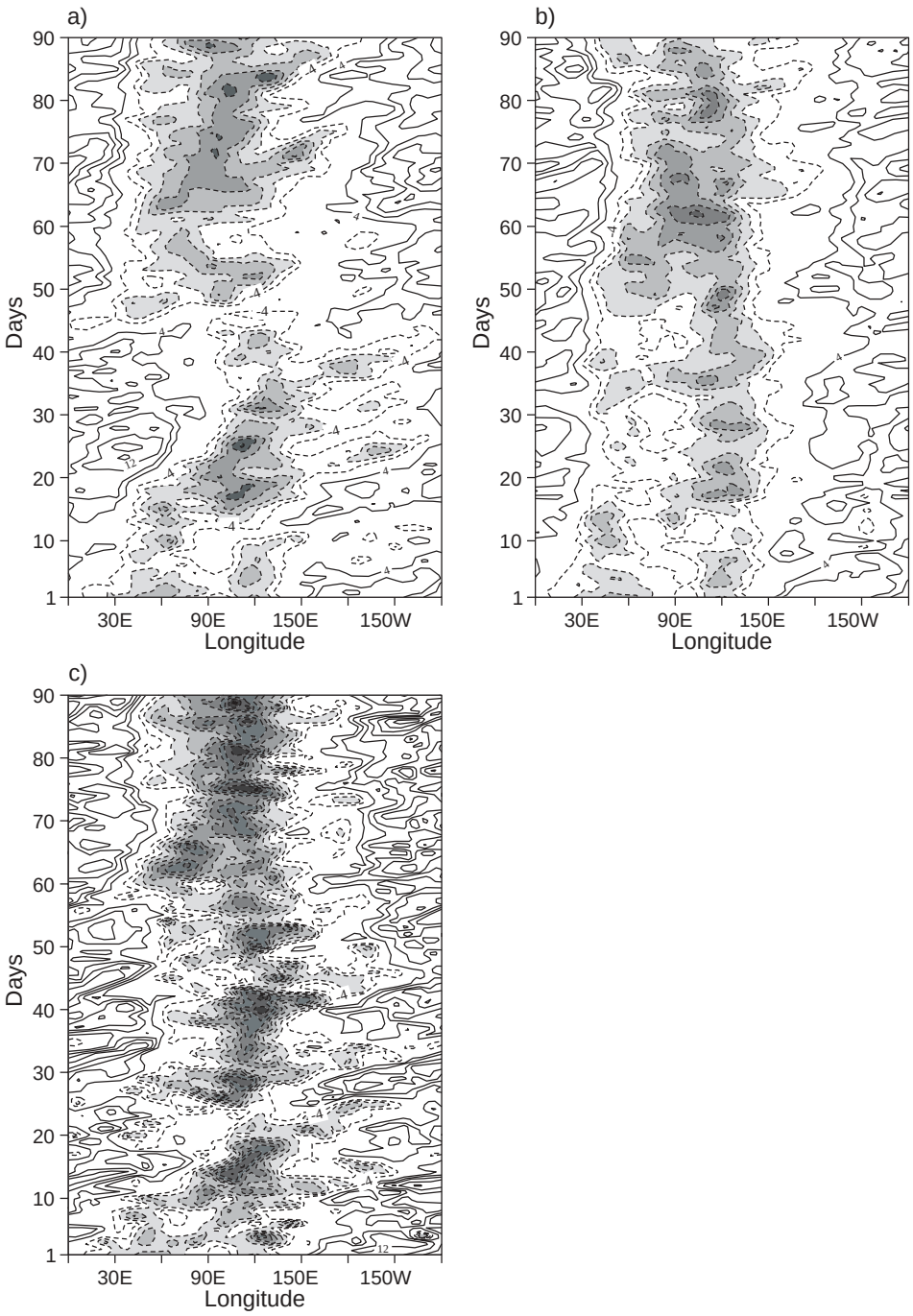

Figure 4: Time evolution of 200 hPa velocity potential over the tropical Indian and Pacific Oceans in a) ECMWF operational analysis from 1 May 1997 to 31 July 1997, b) an ensemble member from the C_control experiment starting on 1 May 1997, and c) an ensemble member from the C_cape experiment starting on 1 May 1997. The velocity potential has been averaged from 10S to 10N. The zonal mean has been removed. The c.i. is $4m^2s^{-1}x10^{-6}$*. Negative values are shown dashed.*

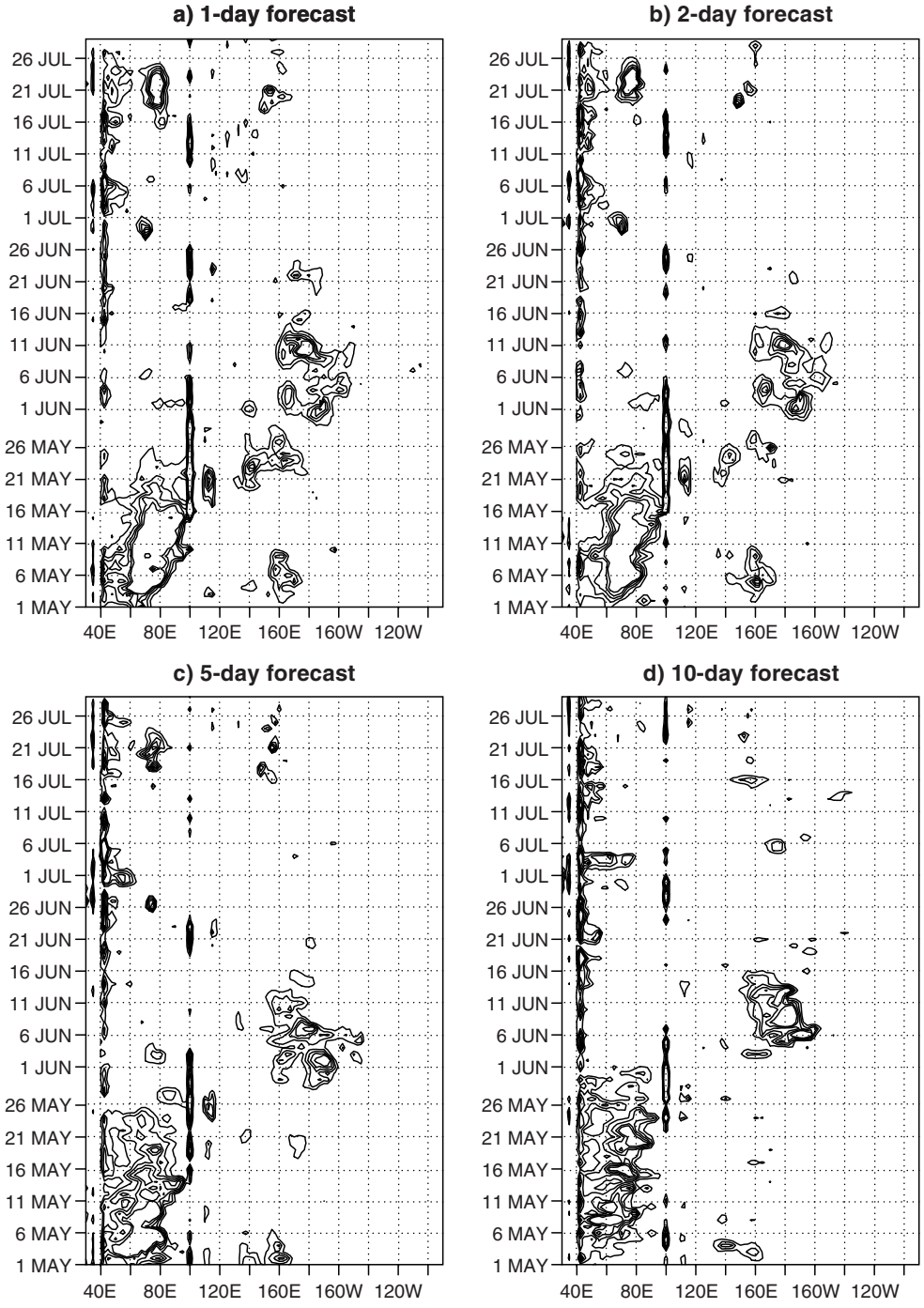

Figure 5: Time evolution of wind stress from a) 1-day, b) 2-day, c) 5-day and d) 10-day forecasts from the ECMWF medium-range operational forecast system. C.i. is $0.02 Nm^{-2}$*. Only positive values are shown, starting at* $0.02 Nm^{-2}$*.*

Experiment	Calibration name	Calibration ens. size	Forecast ens. size
C_control	C_CONTROL_CLIM	30	20 Coupled
C_pert	C_CONTROL_CLIM	30	5 Coupled
C_stoch	C_STOCH_CLIM	30	20 Coupled
C_cape	C_CAPE_CLIM	30	20 Coupled
S_control	S_CONTROL_CLIM	30	20 Semi-coupled
S_cape	S_CAPE_CLIM	30	20 Semi-coupled

Table 1: Summary of coupled experiments

for the model forecasts, which allows the removal of model drift. A 20-member ensemble is started on 1st May 1997 to create the forecasts. The initial conditions on 1st May are obtained from the operational atmospheric and oceanic analysis systems. The ensemble is created by perturbing the initial SST by a small amount. This set of experiments is called C_control.

For forecasts started on 1 May 1997, not one single member of the 20-member ensemble of coupled integrations was able to produce propagating wind events as strong as the observed westerly wind event of May-June 1997 (one particular ensemble member is shown in Figure 3b). There is no eastward propagation of the wind event contained in the initial conditions over the Indian Ocean in any ensemble member. The forecast NINO3 SST anomalies, evaluated relative to C_CONTROL_CLIM, are significantly lower than observed by more than 1K after 3 months of integration (Figure 6), indicating that this new version of the coupled model underpredicts the ENSO development just as the operational seasonal forecasting system shown in Figure 1.

Although much attention has been devoted to the February wind events (for example McPhaden 1999), the wind event in May-June was also very large. It originated in the far western Indian Ocean in April, traversed the Indian Ocean in May, weakened when it reached the Pacific but reintensified in June. Indeed part of this westerly wind event passed far into the eastern Pacific. The impact on the ocean state was considerable. Fig 7 shows the equatorial evolution of analysed anomalies of SST, sea level, wind stress and heat flux for May, June and July 1997. (The SST, wind stress and heat flux data comes from the ECMWF atmospheric analysis system. The sea level is taken from an ocean analysis in which thermal data have been assimilated. The anomalies are computed relative to the corresponding 1991-6 analyzed climatology.) The sea level evolution shows eastward propagation of a Kelvin wave generated by the intense westerly wind anomaly in the west Pacific (around 160E-170E) at the beginning of June. The arrival of this wave in the eastern Pacific coincides with the intensification of the SST anomaly. Could the absence of this wind anomaly in the coupled integrations account for the poor forecasts shown in figures 1 and 6?

An additional five-member ensemble experiment (C_pert) starting on 1st May 1997 is generated in a similar way to C_control, starting from exactly the same atmospheric and ocean initial conditions. The wind stress values from the atmospheric component of the coupled model are augmented by the observed wind stress anomalies computed from the ECMWF analysis over the tropical Pacific (120E-90W, 20N-20S) shown in fig 7c.

Fig 8a shows the difference in sea level between the ensemble-means of the two coupled experiments C_pert and C_control. One can see a signal propagating eastward at approximately $3ms^{-1}$, close to the Kelvin wave speed of the first baroclinic mode. This signal is able to penetrate to the eastern boundary. The sea surface temperature plotted in Figure 8b also shows some sign of this signal but does not show such clear propagation. Indeed after the passage of the Kelvin wave the signal is almost a standing response. The slower behaviour of the SST signal relative to sea level or depth of the 20^o isotherm is well known (Barnett et al 1993). The SST signal does not extend to the eastern boundary.

The amplitude of the SST response reaches in excess of 1.5 K, though the signal averaged over the NINO3

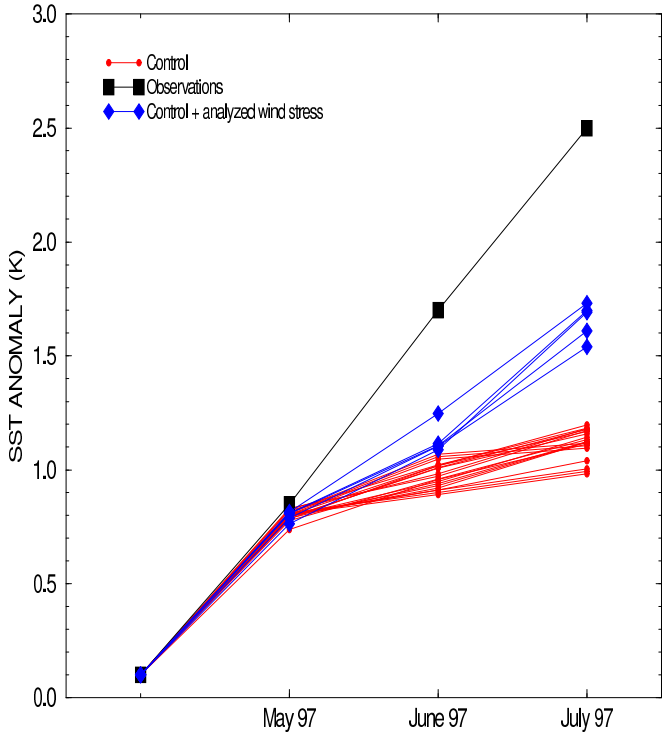

Figure 6: Plume of monthly mean SST anomalies predicted for the NINO3 region. Forecasts start on 1st May 1997, and the 20-member ensemble is generated by adding small perturbations to the initial SSTs. The squares represent the observed values, the circles represent the ensemble distribution for the experiment C_control, and the diamonds represent the ensemble distribution for C_pert. The values are plotted at the middle of the month.

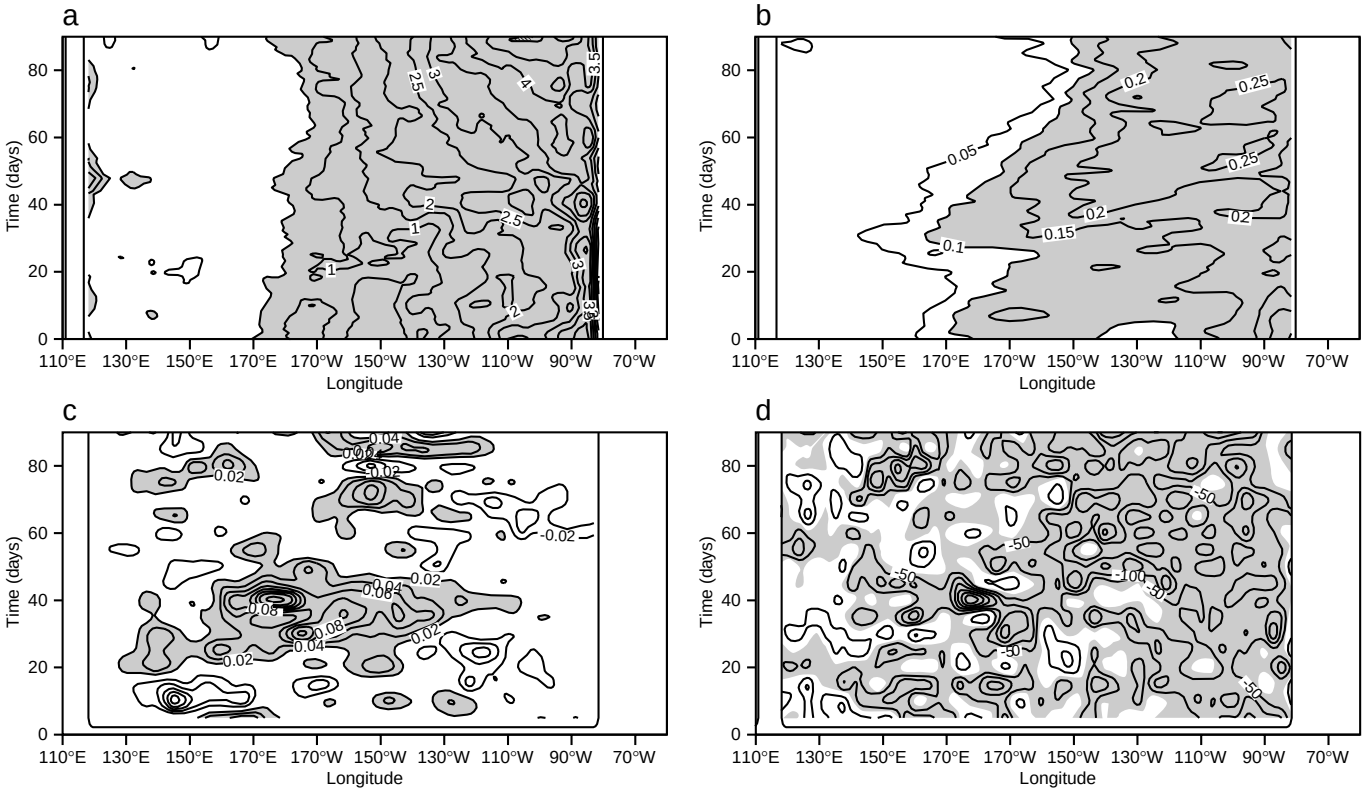

Figure 7: Time evolution (from 1st May 1997 to 1st August 1997) of the analysed anomalies of equatorial a) SST, b) sea level c) zonal wind stress, and d) heat flux; all are with respect to the analyzed 1991-1996 climatology. Only the Pacific basin is shown. c.i. is 0.5K, 0.5m, 0.02 Nm^{-2}, and 50Wm^{-2} respectively. Values above 0.5K, 0.1m, 0.02 Nm^{-2} are shaded in panels a,b and c. Negative values are shaded in panel d.

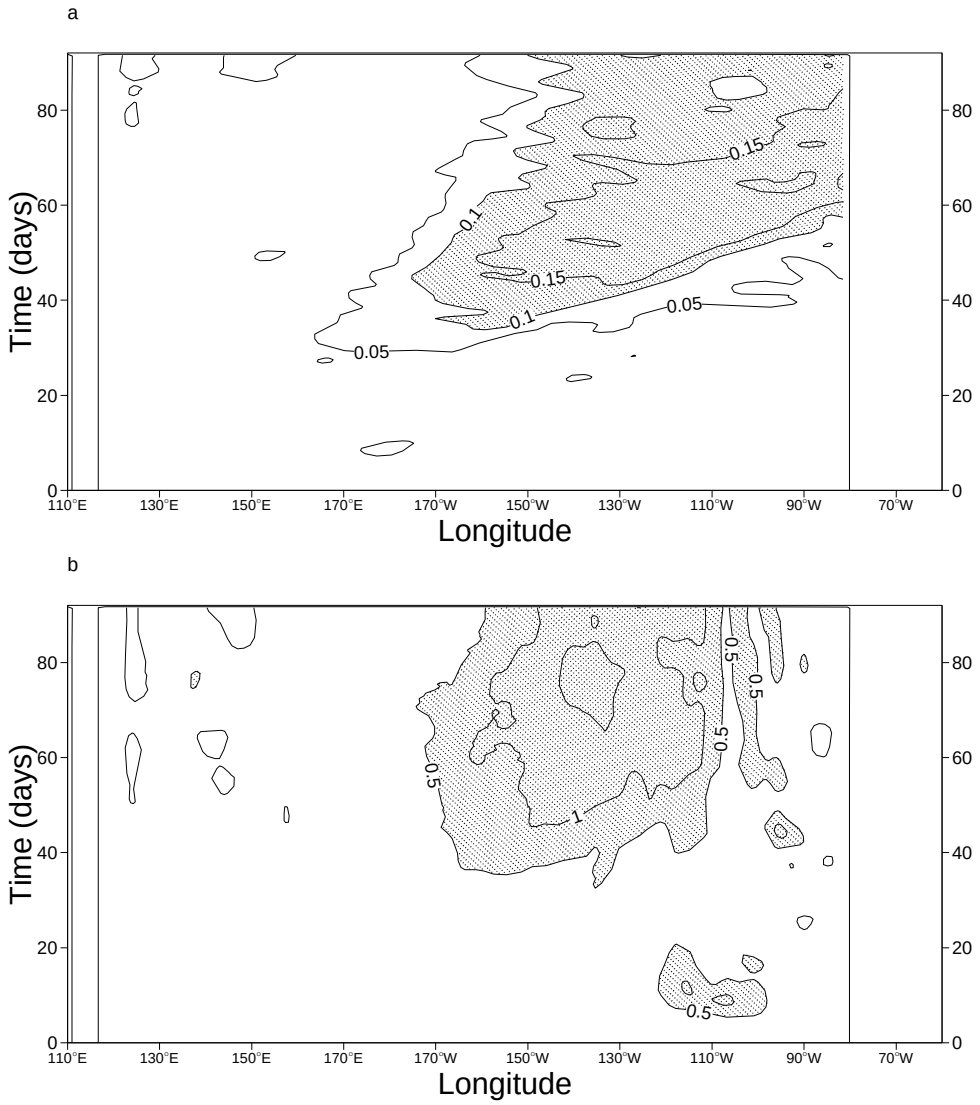

Figure 8: a) Time evolution of ensemble mean difference in equatorial Pacific sea surface height (m) between C_pert and C_control. Start date is 1st May 1997. Shading indicates values greater than 0.1m. c.i. is 0.05m. b) As for (a) but for potential temperature. Shading indicates values greater than 0.5K. c.i. is 0.5K

region is less than this value since it includes a region where the SST signal is weak. Figure 6 shows the predicted SST anomalies in NINO3 from the coupled experiment C_pert. One can see that the latter forecasts are considerably better than those in C_control but are still weaker than the observed amplitude.

The changes in SST induced by the imposed winds in turn generate new winds and heat fluxes. Figures 9a and 9b show the changes in wind and heat flux induced by the SSTs resulting from the wind perturbation, and illustrate the character of the coupled interactions in the model. Over the Central and Eastern Pacific, the stresses are broadly in line with expectation in that there is anomalous convergence over the area of warm SST anomalies. The effect of these winds on SST will be discussed in secn 5.2.

One might have guessed that the development of such a large El-Niño as 1997 would have had some help from the heat fluxes during the development phase (i.e. a positive heat flux anomaly) but it appears that this was not so in the coupled model. The observed SST and heat flux anomalies from the ECMWF analysis system are shown in figures 7a and 7d respectively. They confirm that the heat flux was negative throughout this period. The ratio between heat flux anomalies and SST anomalies for the C_pert experiment is about $-80 W m^{-2} K^{-1}$ over the eastern Pacific, with a close link between the regions of maximum anomalous SST and maximum heat flux (cf figs 8b and 9b). The spatial structure of the analysed heat flux in fig 7d does not mirror the SST anomaly of Figure 7a to the same extent as in the C_pert experiment, and the link between anomalous SST and anomalous heat flux in the analysis seems weaker than in the coupled model, at about $-40 W m^{-2} K^{-1}$, suggesting that the negative feedback from the heat flux in the coupled model may be too strong. The role of heat fluxes will be discussed further in Section 5.

The above experiments suggest that the westerly wind event of June 1997 had a significant impact on the intensification of the 1997 El-Niño and that part of the failure of the coupled GCM to predict the strength of the El-Niño event can be explained by its inability to produce a significant variability in the wind stress forcing. This result does not exclude the possibility that errors in the ocean model, in the model climatology (which is defined from only six different years) or errors in the initial conditions are also important contributions to the inaccuracy of seasonal predictions. The effects of 'additional' errors will not be discussed further in this section since the main focus is to find if there is any relationship between the warming in the NINO3 region and the May-June westerly wind event.

The previous experiments suggest that it is necessary for the atmospheric model to simulate westerly wind events in order to be successful in simulating the intensification of the 1997 El-Niño event. Several methods of increasing the model variability are possible. One consists of adding stochastic perturbations to each member of the ensemble throughout the duration of the forecast. An example of such a technique is the use of stochastic physics (Palmer 2001), where tendencies in the atmospheric model are randomly perturbed. A 20 member ensemble of forecasts with stochastic physics was performed starting on the first of May 1997. This will be denoted C_stoch. Since stochastic physics might perturb the model reference climatology, a new set of hindcasts spanning the period 1991-6 was necessary. This climatology is denoted C_STOCH_CLIM. The 97 anomalies measured relative to this climatology are shown in fig 10a. Comparison with fig 6 indicates a spread of C_stoch ensemble much larger than in the C_control. Several members of the ensemble display a warming stronger than any member of the C_control run, and not too far from the warming obtained when adding observed wind perturbations. No member approaches the observed warming, however.

While stochastic physics creates perturbations of the surface wind, it is unlikely that these will resemble westerly wind events. Stochastic physics perturbations would be applied independently of the fact that we know there will be a westerly wind event, and therefore a part of the predictability is lost. Modifying the physics of the atmospheric model in such a way that it can create and maintain westerly wind events should be a better approach, since any predictability of westerly wind events would then be taken into account. The next section explores this approach.

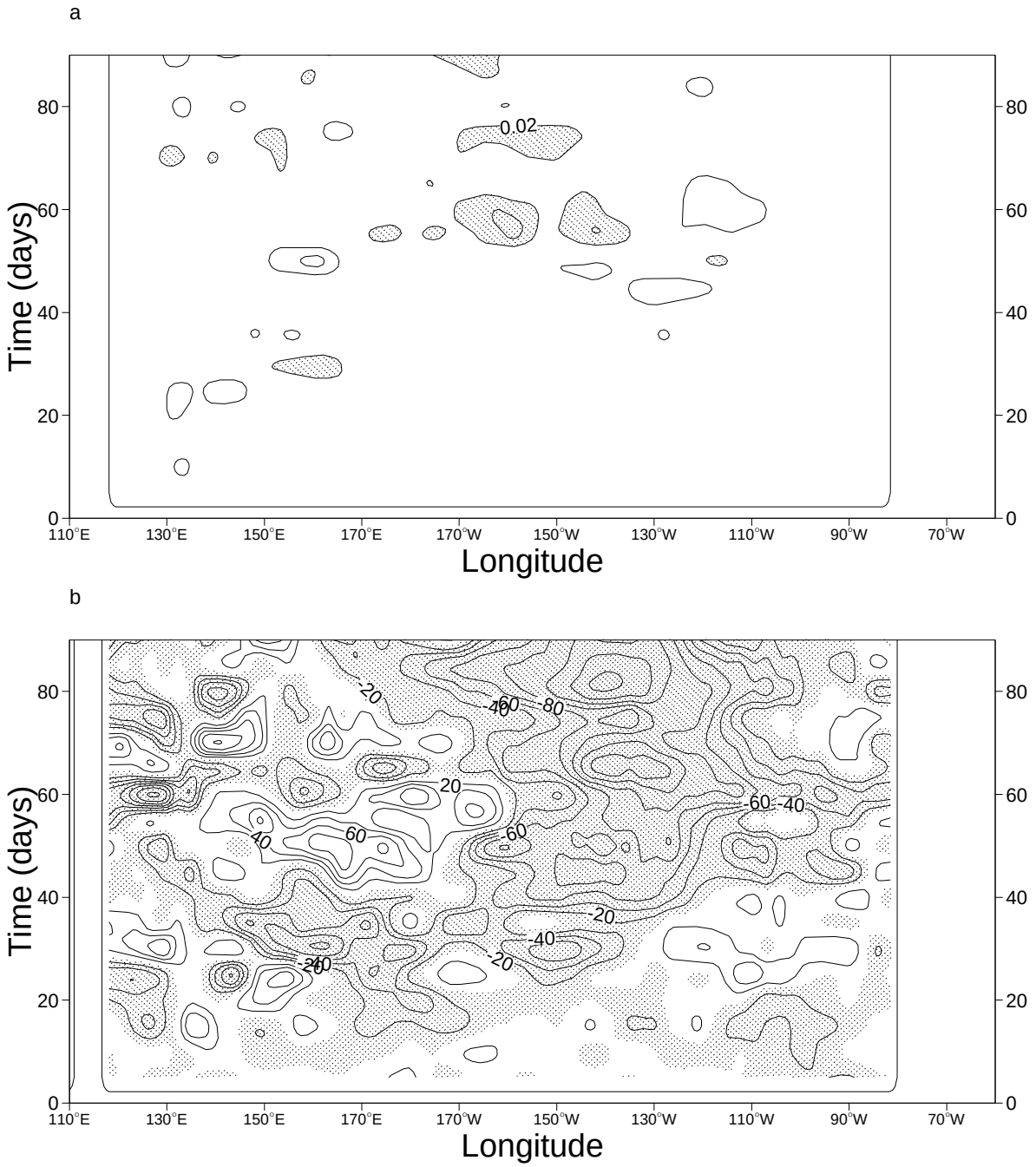

Figure 9: Equatorial Hovmuller diagram of the coupled response to the wind perturbation (τ_{pert}). a) Coupled response in terms of zonal wind stress (τ), defined as $\tau_{C\_pert} - (\tau_{C\_control} + \tau_{pert})$. b) The heat flux ($Hflx$) coupled response, defined as $Hflx_{C\_pert} - Hflx_{C\_control}$. Plots show the average of 5 ensemble members. In a) shading indicates values greater than $0.02 Nm^{-2}$ and the c.i. is $0.02 Nm^{-2}$. In b) negative values are shaded and the c.i. is $20 Wm^{-2}$.

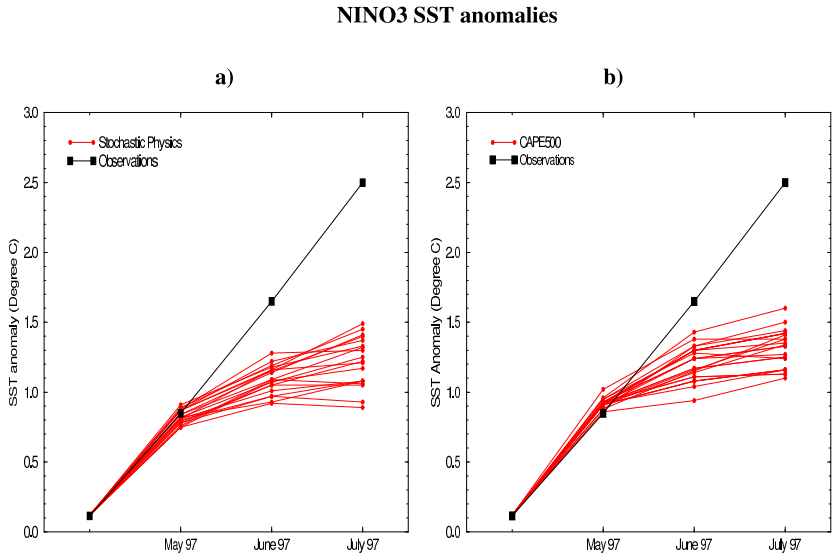

Figure 10: Plume of monthly mean SST anomalies predicted for the NINO3 region ($5^oS - 5^oN$, $90^o - 150^oW$). Forecasts are initialized on 1st May 1997, and the 20-member ensemble is for experiments a) C_stoch and b) C_cape. The squares represent the observed values.

4 Sensitivity of coupled forecasts to changes in cumulus parameterization

The deep convection scheme used in the present model is a mass-flux scheme described in Tiedtke(1989). The scheme is designed to minimize the Convective Available Potential Energy (CAPE), the closure being the condition that the CAPE should be zero. There is no observational evidence that such a condition should apply in the real world. Increasing the threshold of the CAPE is known to significantly impact the transients in the model (Tokioka 1988, Vitart et al 2001). Lin and Neelin (2000) have proposed using different values of the CAPE threshold to generate an ensemble of perturbations. Tests with different values of CAPE threshold indicate that the change in the convective parameterization becomes significant when the CAPE threshold exceeds a value of the order of $200JKg^{-1}$. As the main focus of the following experiments is to find out if the variability of the ECMWF model is sensitive to the CAPE threshold, a value of $500JKg^{-1}$ was chosen, though this may be higher than can be rigorously justified. The choice of $500JKg^{-1}$ for the CAPE thershold will be referred as CAPE500 hereafter.

Part of the failure of the present system to develop intraseasonal variability may be due to the fact that the simulated atmosphere is too stable. Having a CAPE threshold greater than zero delays the onset of deep convective adjustment parametrisation allowing the model to become more unstable and to perform more of this role explicitly. This may help the model to develop intraseasonal variability.

4.1 Results from coupled integrations

As for the previous experiments, a 20-member-ensemble of 3-month integrations starting on 1st May 1997 has been generated with the CAPE500 choice (C_cape runs). In addition, a calibration set consisting of 5-

member ensembles of coupled integrations using the same CAPE500 threshold and starting on 1st May 1991 to 1996 has been created to sample the related climatology C_CAPE_CLIM. Changes in the physics of the model have a significant impact on the mean state and on the drift of the coupled model. For example, the SST of C_CAPE_CLIM is colder than that of C_CONTROL_CLIM in the NINO3 region (Fig. 11). The atmospheric mean state simulated by the C_CAPE_CLIM is not significantly better than the one from the C_CONTROL_CLIM. The impact of delaying the convective activity depends on the season. Additional experimentation based on uncoupled simulations has shown that winter CAPE500 simulations have an improved mean atmospheric circulation but those started in spring-summer showed a degraded mean circulation.

The C_cape experiments increase significantly the variability of the wind stress over the tropical Pacific. Whereas the C_control runs were unable to create strong eastward propagation of wind events in the Central western Pacific, C_cape runs can create westerly wind events near the dateline with an amplitude comparable to observations. Fig. 3c shows one such example. The eastward propagation can also be seen in terms of velocity potential at 200hPa from a coupled C_cape integration starting on 1st May 1997 (fig 4c). The eastward displacement of deep convection in the Tropical Pacific is reminiscent of the Madden-Julian Oscillation, though the speed of propagation is too large. This seems to be a clear improvement in comparison to experiment C_control (fig 4b), though still not fully realistic. However, not a single member of the 20-member ensemble of C_cape started on 1 May 1997 creates a westerly wind event extending as far eastward as observed in June 1997. Nevertheless, the C_cape experiments can be used as sensitivity experiments to evaluate the impact of westerly events on the SST variability. The 20-member C_cape ensemble initiated on 1st May 1997 shown in Figure 10b displays a warming of SST significantly larger than the control ensembles (Fig. 6) (95% significant according to the Wilcoxson-Mann-Whitney test, e.g. Wonnacott and Wonnacott 1997) . The ensemble mean is still far from the observed warming, but some members of the ensemble create a warming close to that obtained when the observed westerly wind anomalies are imposed on the ocean.

All 20 members of the ensemble predict westerly wind events in the first two months of integrations, though the intensity and timing varies considerably from one member to the next. The ensemble members that create the strongest warming over NINO3 coincide with the members exhibiting the strongest westerly wind events. Three-month averages of NINO3 SSTs and zonal winds averaged over the Central Pacific region (160E-180E and 5N-5S) are significantly correlated (correlation of 0.7), suggesting that the westerly wind events in the model have a significant impact on the NINO3 SSTs. Fig 12 shows a Hovmuller diagram of the time evolution of the difference in SSTs, sea level and wind stress between the best C_cape and the best C_control (best meaning the ensemble members that produced the strongest warming in the NINO3 region). The difference in NINO3 SSTs between the two sets of experiments can be traced back to the occurrence of two westerly wind events, in May and June, that propagated eastward well beyond the dateline. The impact of those westerly wind events on the ocean state can be seen in the sea level (fig 12b) as eastward propagating Kelvin waves and in the SST warming that appears to the east of the wind anomaly (figure 12c). This suggests that the ability of C_cape simulations to create westerly wind events is the main reason for the improvement in the NINO3 forecasts. Some improvements with C_cape may be due to a different mean state as shown in Figure 11. In the following section, we will consider the impact of the drift, and in section 5.2 we will evaluate the impact of the wind variability produced in C_cape when acting on a different oceanic mean state, with experiments involving ocean-only runs.

4.2 Results from 'semi'-coupled integrations

To evaluate the influence of the SST drift in figure 11 on the NINO3 forecasts shown in figure 10, experiments have been generated in which the atmosphere sees the observed SSTs, whereas the ocean is forced by the fluxes produced by the atmosphere. Two sets of experiments, S_cape and S_control, have been generated with

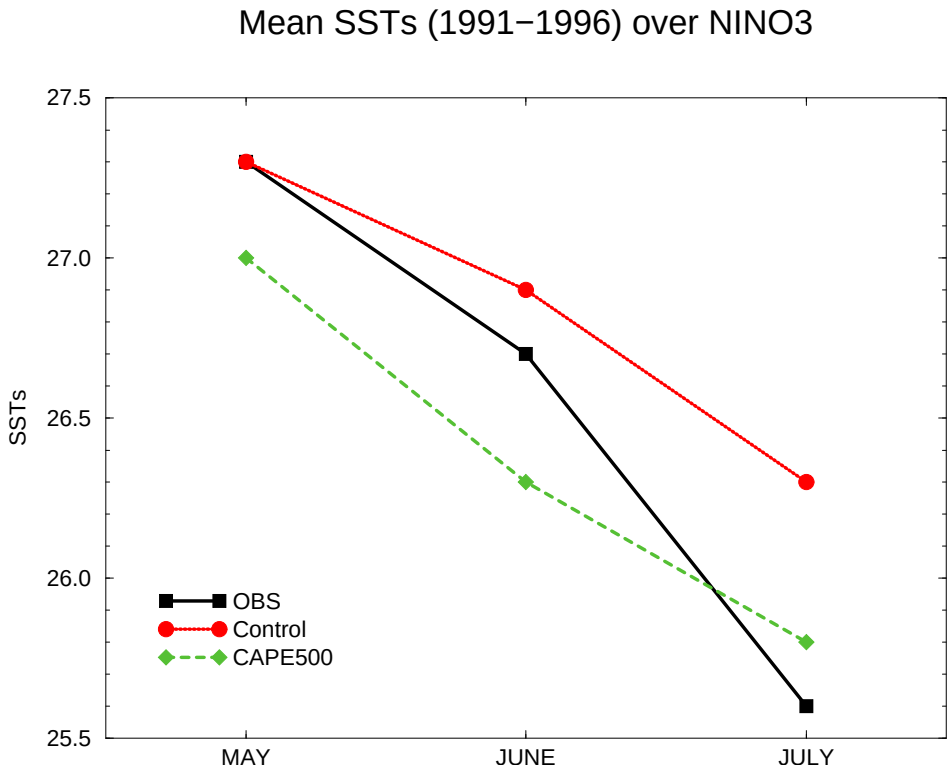

Figure 11: Mean SSTs averaged over the NINO3 region and over the period 1991-1996. The squares represent the observed mean SSTs, the circles, the mean of the C_control integrations starting on 1st May and the diamonds the mean of the C_cape integrations starting on 1st May.

and without the change in the CAPE threshold. The results obtained in this framework are consistent with those obtained when the atmosphere and ocean are fully coupled; i.e. in experiments S_cape the SST warming produced by the ocean model in the NINO3 region is significantly larger than in the corresponding S_control experiments. Since the atmosphere is driven by observed SSTs in these experiments, the drift in SSTs in the ocean model has no impact on the simulated atmospheric intraseasonal variability. Therefore, the difference in the SST anomalies predicted by the ocean model between S_cape and S_control runs does not result from the difference in SST drift.

4.3 Results from uncoupled integrations

In addition to the coupled integrations referred to above, additional experiments using the atmospheric model only and prescribed SSTs have been performed. Some of these were carried out for 'perpetual March' conditions, both for the standard and CAPE500 cumulus parameterizations, and are denoted A_control and A_cape respectively. A major impact of CAPE500 parameteriztion is the significant increase of energy in the 40-50 day band apparent in the A_cape integrations. A power spectrum of equatorial velocity potential from A_cape runs shows a relative maximum for variations with periods around 40 days, not too far from the observed period of the Madden-Julian oscillation (Fig. 13). Results from the A_control integration are also shown for comparison. A less desirable feature in the A_cape integrations is the increase in energy at periods shorter than 10 days.

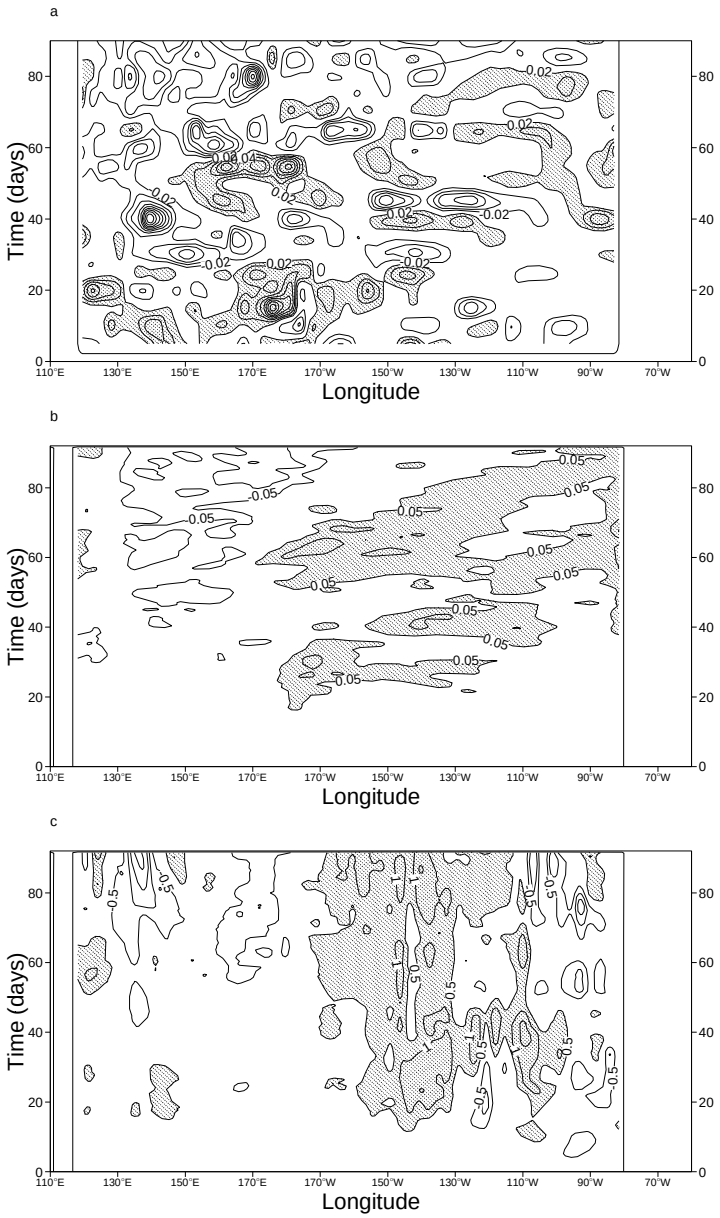

Figure 12: Time evolution of the differences between the best C_cape and the best C_control anomalies of a) surface stress, b) sea level and c) potential temperature. The best member is the one which gives the strongest warming over the NINO3 region. In a) the c.i. is 0.02Nm^{-2} and values greater than 0.02Nm^{-2} are shaded, in b) the c.i. is 0.05m, with values greater than 0.05m shaded, and in c) the c.i. is 0.5K with values larger than 0.5K shaded.

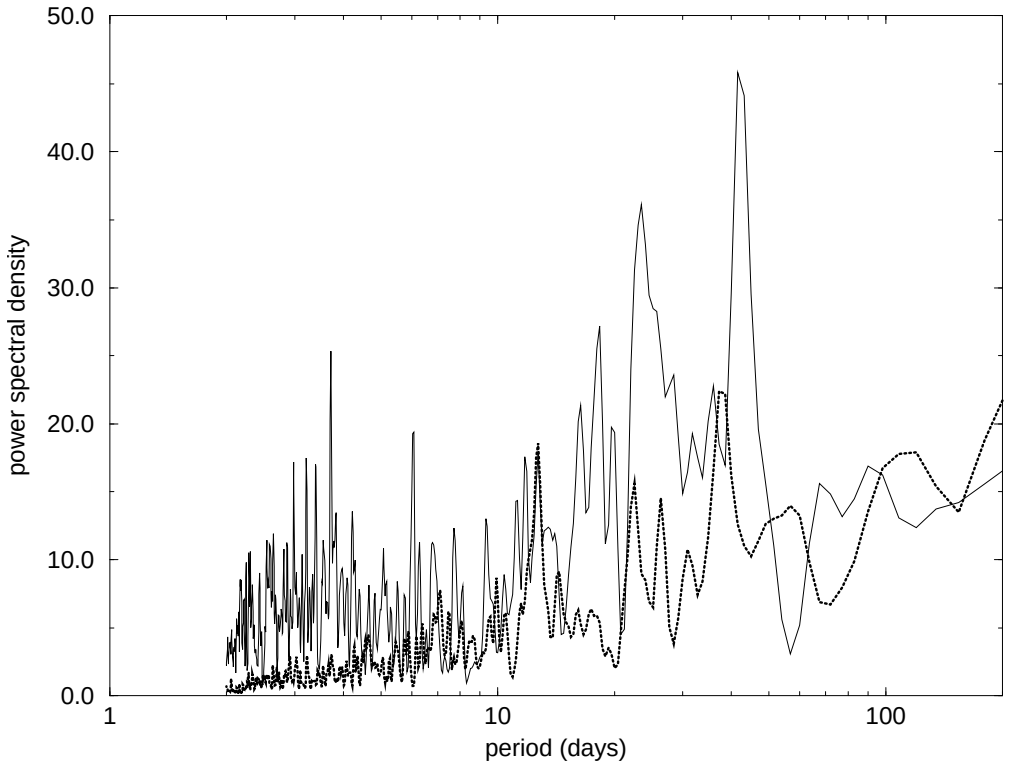

Figure 13: Zonal wave number one equatorial velocity potential computed from 3-year perpetual-March integrations of the atmospheric model using March SSTs. The A_control run is the heavy dotted line and A_cape is the thin full line.

4.4 Conclusions from CAPE experiments

The previous sections have discussed the impact of westerly wind events on the SST in the Niño3 region in 1997. Modifying the convective cumulus parameterization in such a way that it produces a more realistic spectrum of westerly wind events, improves significantly the forecast for the year 1997. However, the overall skill over the period 1991-1996 appears similar for C_control and C_cape experiments, with comparable linear correlation and RMS error when compared with observations.

All 20 members of the C_cape forecast ensemble produce westerly wind events when started on 1st May 1997, although their intensity and timing vary considerably from one member of the ensemble to another. Interestingly, C_cape runs do not systematically produce westerly wind events over the earlier period 1991-1996. This suggests that the westerly wind events in May-June 1997 may have some predictability, and may explain why the C_cape experiment produces better forecasts for 1997 than stochastic physics. Ensembles with stochastic physics present a larger spread than the C_cape ensemble, since it includes the possibility that there are westerly wind events or there are no westerly wind events. The best forecast with stochastic physics is comparable to the best forecast with CAPE500, but the worst forecast with stochastic physics, which does not include any westerly wind event, is clearly worse than the worst forecast with CAPE500. An ensemble of integrations with both stochastic physics and a 500 J/Kg CAPE threshold produces results comparable to the results of the experiment with stochastic physics alone, and therefore worse than with CAPE500 alone. Therefore, stochastic physics seems to have a positive impact on the NINO3 SST forecasts when the atmospheric model does not display any significant intraseasonal variability in the wind stress, but may lower the skill of the forecasts when the model displays some skill in simulating westerly wind events.

5 Ocean-Only experiments

In this section will consider the impact of the wind anomalies in the context of ocean-only experiments. In addition the impact of different components can be quantified by modifying the forcing fields to isolate the component of interest. First, in secn 5.1, we will consider ocean experiments in which we use fluxes from the atmospheric analysis system and initial conditions from the ocean analysis system. Then, in secn 5.2, we will discuss experiments using fluxes from the coupled experiments.

5.1 The ocean response to the observed anomalous conditions

In order to quantify the effect on the SST of the different anomalous conditions observed during May-July 1997, a series of ocean-only experiments was conducted, in which the ocean model was forced using different surface fluxes and ocean initial states. Each integration started on the 1st of May 1997 and lasted for 3 months. To create a reference climatology (FOR_CLIM), the ocean model was forced by analyzed fluxes for 3 months starting from the first of May of each year during the period 1991-1996. The ocean initial conditions were the same as those used in the coupled experiments. This way of creating a forecast and a reference climatology mimics the method used in the coupled experiments. The forcing fields consisted of wind stress, heat and fresh water fluxes derived from ECMWF reanalysis till December 1993 and from NWP operational analysis thereafter (denoted ERA/ops). A summary of the experiments conducted is given in Table 2.

In experiment O_anal, which acts as a control experiment, the forcing is the analysed forcing for May, June, July 97 and the ocean initial conditions are those for 1 May 1997. This represents the best possible attempt to reproduce the observed SSTs. The anomalous wind and heat flux are shown in figures 7c and 7d respectively. If the forcing, the ocean model, the initial conditions and the climatology (FOR_CLIM) were all perfect, the resulting SST anomaly in the forced ocean integration would be equal to that observed. By comparing the SST anomaly from experiment O_anal with the analysed SST anomaly (fig14a with fig 7a), one can see that this is not the case: the ocean model produces an SST signal that peaks at a longitude around 125W compared to 100W in the observations, and its maximum is about 1K weaker than observed. In the west Pacific a cold anomaly of 0.5K to 1K is present in fig 14a which is not present in the observations. On the other hand, we find that the intensity of the sea level and thermocline anomalies in experiment O_anal are in good agreement with the anomalies in the ocean analyses in which all thermal data have been assimilated: the magnitude of the errors is about 2cm in sea level and 10m in thermocline depth, i.e. less than 10% the value of the interannual anomaly. If we take the ocean analysis as a measure of truth, then, since the model reproduces well the analysed sea level and thermocline depth anomalies, we conclude that the dynamical response of the model to the interannual variability of the wind is largely correct. A visual inspection of the anomalous subsurface temperature indicates that the difference between experiment O_anal and the observed state is confined to the upper 50 metres, suggesting that the deficiencies in the simulation of the SST anomalies may be attributed to surface processes such as heat fluxes and/or mixing within the mixed layer.

The SST anomaly produced by the model is the response to 4 different anomalous conditions: wind stress, heat flux, fresh water and initial conditions. To quantify the contribution of each of these to the evolution of SST we have carried out 4 different experiments O_notaux, O_nohflx, O_nopme and O_nooic, in which the effect of withdrawing the component in question is assessed by replacing the anomalous conditions over the tropical Pacific within 20 degrees of the equator by their corresponding climatological values.

The contribution of the anomalous wind can be measured by comparing experiment O_anal with experiment O_notaux. Figure 14b shows the SST differences between these 2 experiments. The effect of the wind is only apparent after 40 days into the integration. The peak value of the SST difference is greater than 3.5K in the

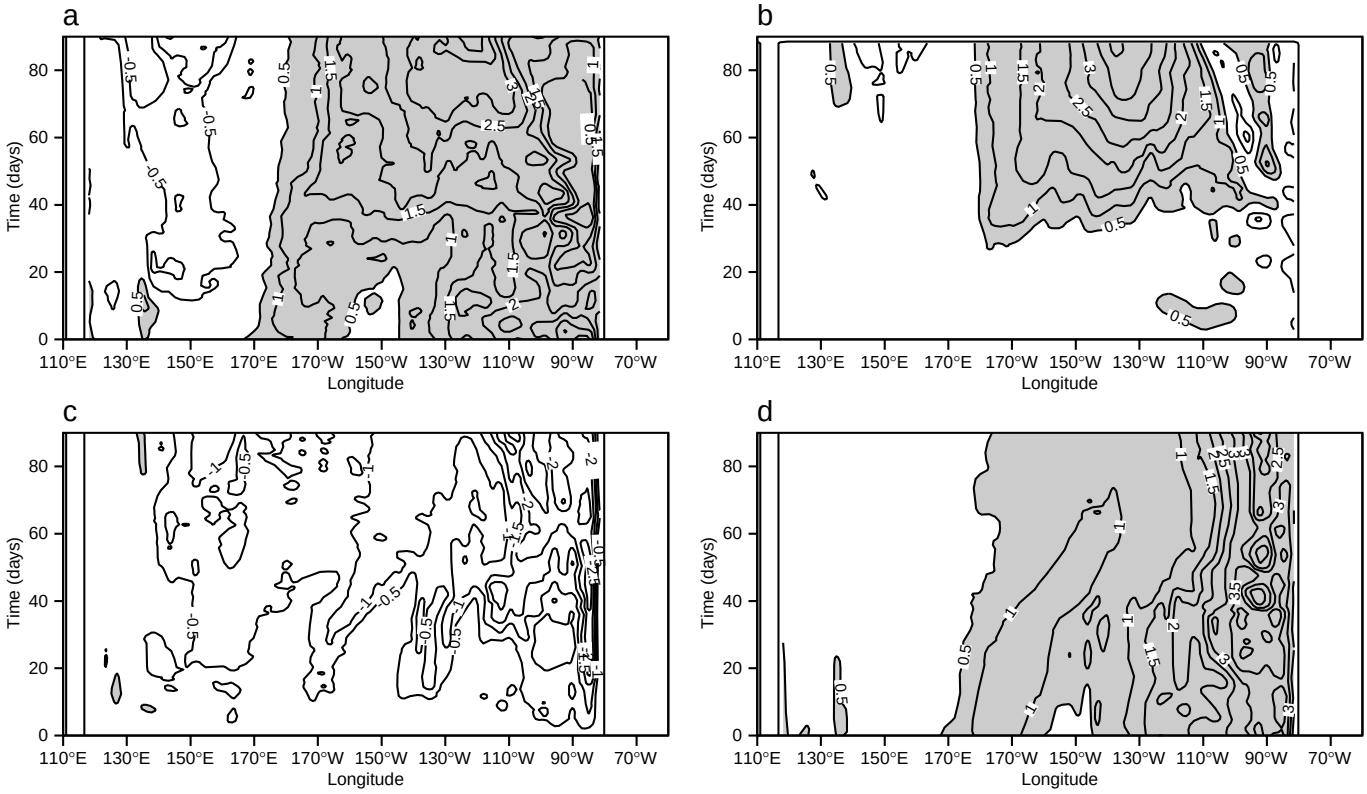

Figure 14: Time evolution of the differences in equatorial SST between: a) O_anal and FOR_CLIM. b) O_anal and O_notaux, c) O_anal and O_nohflx, d) O_anal and O_nooic. The c.i. is 0.5K. Values greater than 0.5K are shaded.

Experiment	Wind	Heat	P-E	Ocean I.C	Comparison
O_anal	Analysis	Analysis	Analysis	Analysis	FOR_CLIM
O_notaux	clim	Analysis	Analysis	Analysis	O_anal
O_nohflx	Analysis	clim	Analysis	Analysis	O_anal
O_nopme	Analysis	Analysis	clim	Analysis	O_anal
O_nooic	Analysis	Analysis	Analysis	clim	O_anal

Table 2: Summary of ocean-only experiments conducted to measure the impact of the different anomalous conditions on SST evolution during May, June, July 1997. In the table, "clim" stands for the 1991-1996 climatology of the given variable.

Experiment	Wind Anomaly	Heat Anomaly	Forcing Climatology
C_control	C_control	C_control	C_CONTROL_CLIM
Ocx_ch	C_control	C_control	FOR_CLIM
Ocx	C_control	Analysis	FOR_CLIM
Oc500x	C_cape	Analysis	FOR_CLIM
Oix	See fig 9a	Analysis	FOR_CLIM
Oih	Analysis	See fig 9b	FOR_CLIM

Table 3: Summary of ocean-only experiments conducted to isolate the impact of the different components of coupled fluxes. Each experiment consists of an ensemble of 5 ocean integrations.

central eastern Pacific and is comparable to that from the combined contribution of heat, wind stress, P-E and initial conditions shown in fig 14a. As one expects the heat flux to have a damping effect and the effect of P-E to be small, this suggests that the anomalies in the ocean initial conditions are important not only during the first 40 days but that their influence extends throughout the integration. In the western Pacific the wind does not seem to be responsible for the cooling noted in fig 14a.

In experiment O_nohflx, the heat flux anomaly over the tropical Pacific has been removed, and therefore only climatological heat flux is used over this area; in all other respects it is like experiment O_anal. The contribution of the anomalous heat flux to the SST, as measured by the difference between experiment O_anal and O_nohflx, is shown in figure 14c. As anticipated, the heat fluxes have a damping effect, which is particularly strong in the eastern Pacific, over the area of maximum observed SST anomaly shown in figure 7a. The cooling induced in the far east reaches 2.5 K. In the eastern Pacific the pattern of influence of the heat flux on SST is similar to the error in SST in experiment O_anal (fig 14a-fig7a), suggesting that the anomalous heat flux from the atmospheric analysis might be in error. The effect of the heat flux anomaly, however, is not restricted to the eastern Pacific, but extends westward as far as 140E, producing a cooling of 1K around 155E during the 3rd month. The average effect of the heat flux is to produce an overall cooling of 0.5K in SST, but its effect on other fields such as sea level and depth of the 20 degree isotherm (D20) is small.

The effect of the anomalous ocean initial conditions can be measured by the difference between experiment O_anal and 0_nooic. This latter uses the climatological mean state for the ocean obtained by averaging the ocean initial states for the 1st of May for each year from 1991 to 1996. Figure 14d shows that the anomalous ocean initial conditions contributes to the SST warming all along the equator with a maximum contribution of 3-3.5 K east of 110W. As earlier suggested, this figure indicates that the effect of the initial conditions extends throughout the integration.

As expected, the effect of the anomalous P-E forcing is small in all the fields, namely less than 0.2K in SST, less than 2cm in the sea level and less than 5m in D20, and so is not shown.

5.2 The ocean response to forcing from coupled experiments

In sections 2 and 3 we described how the coupled model underpredicted the full intensity of the SST anomaly, and assessed the model sensitivity to wind perturbations. The results suggested that the failure of the coupled model to forecast the correct SST amplitude was largely due to the lack of wind variability. However, figure 6 showed that even when the full wind stress anomaly was included, the SST anomaly was still underpredicted by the coupled model. Further, in the previous section we showed the SST response to the anomalous wind stress in the ocean-only experiments (3.5K, figure 14b) was more than double the response obtained in the coupled experiment C_pert (1.5K, fig 8b). These facts point to other deficiencies in the coupled model. For example a different ocean mean state in the coupled system can influence the wave propagation as suggested by Benestad et al (2002). Additional coupled interactions can result from changes in the SST. Therefore, an additional set of experiments was conducted in ocean-only mode, in which the anomalous atmospheric forcing from the coupled model experiments was superimposed on the climatological forcing FOR_CLIM. A first set of experiments was designed to measure the nonlinear effects of the ocean mean state of the coupled model on the development of SST anomaly, both for the control runs and for the CAPE500 experiments. A second set was designed to quantify the strength of the "coupled interactions". A summary of these experiments is given in Table 3.

To measure the nonlinear impact of the ocean mean state of experiment C_control on the SST evolution, experiment Ocx_ch was carried out, in which both the anomalous wind stress and heat fluxes from 5 ensemble members of the coupled integrations C_control are superimposed on the analyzed flux climatology (FOR_CLIM). Experiments C_control and Ocx_ch have therefore the same anomalous forcing (in terms of wind and momentum), superimposed on different mean flux climatologies (C_CONTROL_CLIM and FOR_CLIM respectively). Assuming that the effect of P-E on SST is small, the differences between anomalies in Ocx_ch and C_control will be indicative of the effect of the ocean mean state. The anomalies are calculated with respect to their respective oceanic mean states FOR_CLIM and C_CONTROL_CLIM. In the absence of non linear interactions, the anomalies from Ocx_ch and C_control would be identical. Results indicate that the differences between the equatorial SST anomalies from these experiments hardly exceed 0.5K in the central Pacific (figure 15a). The mean state has largest impact in the western Pacific (west of 150E) and in the far eastern Pacific (east of 110W), where the coupled mean state favours the development of larger warm anomalies than the forced mean state. Therefore, it can be concluded that the weak SST response to the wind perturbation in experiment C_pert can not be attributed to the coupled drift.

In section 4.1, we discussed the impact of the CAPE500 parameterization on the coupled model. Results from experiment C_cape showed improved SST anomaly forecasts, likely due to the increase in the atmospheric intraseasonal variability. But there were other factors that could contribute to the differences in SST forecasts, such as the different mean state of the atmosphere, and the different mean state of the ocean. In section 4.2 semi-coupled experiments showed that the increase in intraseasonal variability observed in experiment C_cape was not linked to the different mean state of the atmosphere associated with the drift in SST. To address the impact of the ocean mean state on the improved SST forecasts from experiment C_cape, we need a further set of ocean-only experiments, in which only the anomalous forcing from the coupled integrations is considered. In experiments Ocx and Oc500x, the tropical Pacific wind stress anomalies from 5 ensemble members of the coupled C_control and C_cape experiments (the anomalies computed relative to their own climatologies, C_CONTROL_CLIM and C_CAPE_CLIM) are added to the analyzed climatology FOR_CLIM. In all other respects the experiments are the same, and have the same initial conditions, heat and P-E forcing as experiment O_notaux. The difference between the SST anomalies from these 2 experiments (not shown) is similar to the difference between the anomalies of the corresponding coupled experiments, confirming that the westerly wind events created by the CAPE500 parameterization are instrumental in the improvement of the forecast.

The relative contributions of the wind stress and heat flux resulting from the coupled interactions (and depicted

in figure 9) can be measured in ocean-only experiments. In experiment Oix, the wind stress anomaly shown in fig 9a is added to the FOR_CLIM climatology. In all other respects, it is like experiment O_notaux (where the wind stress was climatology). Differences between these 2 experiments indicate that the wind component of the "coupled" interaction has a small effect: less than 0.5K on the SST over the equatorial region, less than 5m in D20, and less than 2cm in the sea level, and is not shown. The story is different with the heat flux. In experiment Oih, the heat flux component of the "coupled interaction" in figure 9b is added to FOR_CLIM. In all other respects it is like experiment O_nohflx. The difference between these 2 experiments, shown in figure 15b, indicates that the heat flux from the "coupled interaction" cools the SST anomalies by more that 1.5K. This implies that the anomaly from experiment C_pert (and shown in figure 8b) would have been 1.5K larger towards the end of the integration if there had not been any heat flux response to the SST induced by the imposed wind perturbation. The coupled response in terms of heat flux implies a negative feedback, of strength around 80W$m^{-2}K^{-1}$, which may be overestimated by the coupled model, as discussed in section 3.

6 Conclusions

The present paper explores the impact of the 1997 westerly wind event in May/June 1997 on NINO3 forecasts with the ECMWF coupled model. It also evaluates the contributions of the different atmospheric fluxes and ocean initial conditions on the SST warming observed during the period May-July 1997.

Coupled forecasts started on 1 May 1997 underestimate the amplitude of the NINO3 anomalies in July by more than 1K. The coupled model does not produce strong westerly wind events in the central west Pacific, as observed in May-June 1997. An ensemble of coupled ocean-atmosphere integrations where the observed wind stress anomalies over the tropical Pacific have been added to the wind stress from the atmospheric model produces significantly better forecasts over the NINO3 region. The warming in this region exceeds the SSTs in the control run by more than 0.5K, but the perturbed run still underpredicts the full magnitude of the observed SST anomaly. The coupled model response to this warming is characterized by a negative feedback in terms of heat flux, that acts to reduce the SST anomaly.

Experiments in which the threshold for convection of CAPE is increased to 500 J/Kg suggest that improving the representation of transients in the atmospheric component of the GCM significantly improves the forecasts. CAPE500 seems to be beneficial only when westerly wind events significantly impact the NINO3 SSTs, as was the case in 1997. The choice of a 500 J/KG CAPE threshold is probably unrealistically high, but these experiments highlight the importance of simulating westerly wind events in a GCM. The present paper also suggests that stochastically perturbing the model physics significantly improves the seasonal forecast of NINO3 SSTs, but not as much as with the CAPE500 experiment. This is likely due to the fact that, unlike the integrations with stochastic physics, the CAPE500 integrations seem to display an interannual variability in the occurrence of westerly wind events. The CAPE500 experiments exhibited a more intense intraseasonal variability, extending eastward as far as 160E. It would be interesting to determine which aspect of the intraseasonal variablity (intensity, location, frequency band) is most influential in ENSO forecasting. Further, it is important to determine the sensitivity of the SSTs to the intraseasonal variability as a function of the ocean initial conditions. Future plans also include investigating the predictability of westerly wind events in intraseasonal and seasonal scale using the CAPE500 parameterization. This will be discussed in a forthcoming paper.

In the coupled experiments, the absence of westerly wind variability only partially explains why the ECMWF seasonal forecasting system failed to predict the strong warming in the NINO3 region when starting on 1st May 1997. Even when the westerly wind events are included, the NINO3 forecasts are still well below observations. The response to the wind perturbation is stronger in the ocean-only experiments, where no coupled effects are allowed (i.e. variations in heat, momentum and P-E fluxes are excluded). Ocean-only experiments indicate

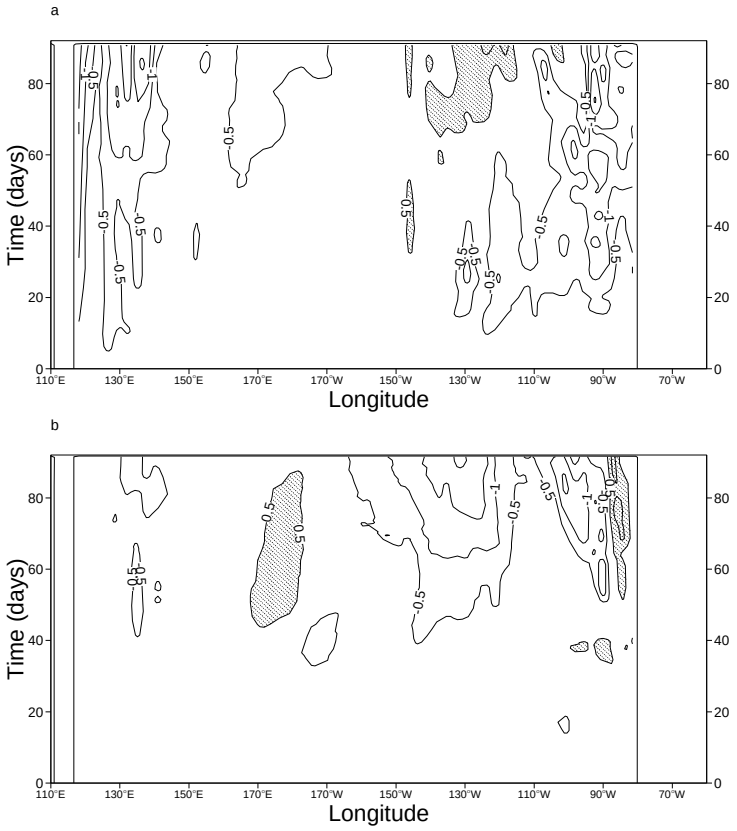

Figure 15: Impact on the evolution of the equatorial SST anomaly of a) the mean state, as measured by the difference between the anomalies from experiment Ocx_ch and experiment C_control (each anomaly referred to its respective climatology). b) the heat flux from the "coupled response" (depicted in figure 9b), as measured by the difference between experiment Oih and O_nohflx. The c.i. is 0.5K, with values over 0.5K shaded.

that the heat flux produced by the coupled model as a response to the SST anomaly causes the equatorial SSTs to cool by more than 1.5K. The ocean-only experiments also indicate the response of the atmosphere to the warming in the eastern Pacific in terms of winds does not produce any significant effect on the SST. The ocean mean state has some impact in the amplitude of the SST generated by the wind pertubation, especially in the far eastern and far western Pacific. However, results from ocean-only experiments indicate that the mean state of ocean model does not explain the weak SST response of the coupled model to the wind perturbations, suggesting that the ocean mean state is not a major contributor to the error in 1st May forecast of NINO3 SST.

Results with ocean-only experiments indicate that the 2 major contributors to the SST warming during May-July 1997 from forecasts initiated the 1st May 1997 were the wind anomaly in the western Pacific and the ocean initial conditions. The anomalous heat flux acted to damp the SST warming, and results suggest that the heat flux estimate might be a source of error in the SST simulation.

REFERENCES

Barnett, T.P., 1984: Origins of the Southern Oscillation. Annual Climate Diagnostics Workshop, Ontario, Canada, NOAA, 155-158.

Barnett,T.P., M. Latif, E. Kirk, E. Roeckner, 1991: On ENSO Physics. *J. Climate*, **4**, 487-515.

Barnett,T.P., M. Latif, N. Graham, M. Flugel, S. Pazan, and W. White, 1993: ENSO and ENSO related Predictability. Part I: Prediction of Equatorial Pacific Sea Surface Temperature with a Hybrid Coupled Ocean-Atmosphere Model. *J. Climate*, **6**,1545-1566.

Barnston, Anthony G., Yuxiang He, Michael H. Glantz, 1999: Predictive Skill of Statistical and Dynamical Climate Models in SST Forecasts during the 1997-98 El-Niño Episode and the 1998 La Niña Onset. *Bull. Amer. Meteor. Soc.*, **80**, 217-244.

Benestad R., R. Sutton and D.L.T. Anderson 2002: The effect of El Niño on intraseasonal Kelvin waves. Quar. J. Royal Met. Soc. In press.

Bergman, J. W., H.H. Hendon, and K.M. Weickmann, 2001: Intraseasonal air-sea interactions at the onset of El-Niño. *J. Climate*, **14**, 1702-1719.

Boulanger, J.-P., E. Durand, J.-P. Duvel, C. Menkes, P. Delecluse, M.Imbard, M. Lengaigne, G. Madec and S. Masson, 2001: Role of non-linear oceanic processes in the response to westerly wind events: new implications for the 1997 El Niño onset. *Geophys. Res. Lett.* , **28** (8), 1603-1606.

Chen, S.S., R.A Houze Jr., and B.E. Mapes, 1996: Multiscale variability of deep convection in relation to large-scale circulation in TOGA COARE. *J. Atmos. Sci.*, **53**, 1380-1409.

Gates, W.L., 1992: AMIP: The atmospheric model intercomparison project. *Bull. Amer. Meteor. Soc.*, **73**, 1962-1970.

Harrison, D.E., 1984: On the appearance of sustained equatorial westerlies during the 1982 Pacific warm event. *Science*, **225**, 1092-1102.

Harrison, D.RE., and and B.S. Giese, 1991: Episodes of surface westerly wind as observed from islands in the western tropical Pacific. *J. Geophys. Res.*, **96**, 3221-3237.

Hendon, H. H., B. Liebmann, and J.D. Glick, 1998: Oceanic Kelvin waves and the Madden-Julian Oscillation. *J. Atmos. Sci.*, **55**, 88-101.

Keen, R.A., 1982: The role of cross-equatorial cyclone pairs in the Southern Oscillation. *Mon. Wea. Rev.*, **110**, 1405-1416.

Kessler, W.S. and R. Kleeman, 2000: Rectification of the Madden-Julian Oscillation into the ENSO cycle. *J.Climate*, **13**, 3560-3575.

Krishnamurti, T. N., D. Bachiochi, T. LaRow, B. Jha, M. Terawi, D.R. Chakraborty, R. Correa-Torres, D. Oosterhof, 2000: Coupled atmosphere-ocean modeling of the El-Niño of 1997-98. *J. Climate*, **13**, 2428-2459.

Landsea, C.W., J.A. Knaff, 2000: How much skill was there in forecasting the very strong 1997-1998 El Niño?. *Bull. Amer. Meteor. Soc.*, **81**, 2107-2120 .

Latif, M., D. Anderson, T. Barnett, M. Cane, R. Kleeman, A. Leetmaa, J.O'Brien, A. Rosati, and E. Schneider, 1998: A review of the predictability and prediction of ENSO. *J. Geophys. Res.*, **103**, 14,375-14,393.

Lin, W.-B. and D.J. Neelin, 2000: Influence of a stochastic moist convective parameterization on tropical

climate variability. *geophys. Res. Lett.*, **27**, 3691-3694.

Lin, X., and R.H. Johnson, 1996: Kinematic and thermodynamic characteristics of the flow over the western Pacific warm pool during TOGA COARE. *J. Atmos. Sci.*, **53**, 695-715.

Madden, R.A., and P.R. Julian, 1971: Detection of a 40-50 day oscillation in the zonal wind in the tropical Pacific. *J. Atmos. Sci.*, **28**: 702-708.

Madden, R.A., and P.R. Julian, 1972: Description of global-scale circulation cells in the tropics with a 40-50 day period. *J. Atmos. Sci*, **29**: 1109-1123.

McPhaden, M.J., 1999: Genesis and evolution of the 1997-98 El Niño, *Science*, **283**, 950-954.

Palmer, T.N., 2001: A nonlinear dynamical perspective on model error: A proposal for non-local stochastic-dynamic parametrization in weather and climate prediction models. *Q.J.R. Meteorol. Soc.*, **127**, 279-304.

Perigaud, C. and C. Cassou, 2000: Importance of oceanic decadal trends and westerly wind bursts for forecasting El Niño. *Geophys. Res. Lett.*, **27**, 389-392.

Reynolds, R.W., and T.M. Smith, 1994: improved global sea surface temperatures analyses using optimum interpolation. *J. Climate*, **7**, 929-948.

Slingo, J.M., 1998: The 1997-98 El Niño. *Weather*, **53**, 274-281.

Slingo, J.M., K.R. Sperber, J.S. Boyle, J.-P. Ceron, M. Dix, B. Dugas, W. Ebizus aki, J. Fyfe, D. Gregory, J.-F. Gueremy, J. Hack, A. Harzallah, P. Inness, A. Kitoh, WK.-M. Lau, B. McAvaney, R. Madden, A. Matthews, T.N. palmer, C.-K. Park, D. Randall, N. Renno, 1996: Intraseasonal oscillations in 15 atmospheric general circulation models: Results from an AMIP diagnostic subproject. *Clim. Dynam.*, **12**, 325-357.

Slingo, J.M., D. P. Rowell, K.R. Sperber, and F. Nortley, 1998: On the predictability of the interannual behaviour of the Madden-Julian Oscillation and its relationship with El-Niño. *Quart. J. Roy. Meteor. Soc.*, **125**, 583-609.

Smith. N., J.E. Blomley, and G. Meyers, 1991: A univariate statistical interpolation scheme for subsurface thermal analyses in the tropical oceans. *Progress in Oceanography*, **28** , Pergamon, 219-256.

Stockdale, T.N., D.L.T. Anderson, J.O.S. Alves, and M.A. Balmaseda, 1998: Global seasonal rainfall forecasts using a coupled-atmosphere model. *Nature*, **392**, 370-373.

Tiedtke, M., 1989: A comprehensive mas-flux scheme for cumulus parameterization in large-scale models. Physically-based modeling and simulation of climate change. Eds M. Schlesinger and D. Reidel, Hingham, Mass. USA. 375-431.

Tokioka, T., K. Yamazaki, A. Kitoh and T. Ose, 1988: The equatorial 30-60 day oscillation and the Arakawa-Schubert penetrative cumulus parameterization. *J. Meteorl. Soc. Jpn.*, **6**, 883-901.

Trenberth, K.E., 1998: Development and forecasts of the 1997-1998 El Niño: CLIVAR scientific issues. Exchanges (CLIVAR newsletter), published by the International CLIVAR project Office, Max-Planck-Institute for Meteorology, Hamburg, Germany.

Vitart. F., J.L. Anderson, J. Sirutis and R.E. Tuleya, 2001: Sensitivity of tropical storms simulated by a general circulation model to changes in cumulus parametrization. *Quart. J. Roy. Meteor. Soc.*, **127**, 25-51.

Wonnacott, T.H., and R. J. Wonnacott, 1977: Introductory to Statistics, John Wiley, 650 pp.

Zhang, C., 1996: Atmospheric intraseasonal variability at the surface in the tropical western Pacific Ocean. *J. Atmos. Sci.*, **53**, 739-758.